HHS Public Access

Author manuscript

*Nat Commun*. Author manuscript; available in PMC 2014 October 09.

Published in final edited form as:

*Nat Commun*. 2013 ; 4: 2540. doi:10.1038/ncomms3540.

# Bio-Inspired Voltage-Dependent Calcium Channel Blockers

**Tingting Yang**[*], **Lin-Ling He**[*], **Ming Chen**, **Kun Fang**, and **Henry M. Colecraft**

Department of Physiology and Cellular Biophysics, Columbia University, College of Physicians and Surgeons, 1150 St. Nicholas Avenue, New York, NY 10032, U.S.A

## Abstract

$Ca^{2+}$ influx via voltage-dependent $Ca_V1/Ca_V2$ channels couples electrical signals to biological responses in excitable cells. $Ca_V1/Ca_V2$ channel blockers have broad biotechnological and therapeutic applications. Here we report a general method for developing novel genetically-encoded calcium channel blockers inspired by Rem, a small G-protein that constitutively inhibits $Ca_V1/Ca_V2$ channels. We show that diverse cytosolic proteins ($Ca_V\beta$, 14-3-3, calmodulin, and CaMKII) that bind pore-forming $\alpha_1$-subunits can be converted into calcium channel blockers with tunable selectivity, kinetics, and potency, simply by anchoring them to the plasma membrane. We term this method "channel inactivation induced by membrane-tethering of an associated protein" (ChIMP). ChIMP is potentially extendable to small-molecule drug discovery, as engineering FK506-binding protein into intracellular sites within $Ca_V1.2$-$\alpha_{1C}$ permits heterodimerization-initiated channel inhibition with rapamycin. The results reveal a universal method for developing novel calcium channel blockers that may be extended to develop probes for a broad cohort of unrelated ion channels.

High-voltage-activated $Ca^{2+}$ ($Ca_V1/Ca_V2$) channels convert membrane electrical signals into $Ca^{2+}$ influx that drives essential processes ranging from muscle contraction to synaptic transmission[1]. $Ca_V1/Ca_V2$ channels are hetero-multimers comprised minimally of any one of seven pore-forming $\alpha_1$ ($Ca_V1.1$–$Ca_V1.4$; $Ca_V2.1$–$Ca_V2.3$), four $Ca_V\beta$ ($Ca_V\beta_1$–$\beta_4$), and four $\alpha_2\delta$ ($\alpha_2\delta1$-$\alpha_2\delta4$) subunits in a 1:1:1 ratio[1,2]. $Ca_V1/Ca_V2$ channel inhibition is an important or potential therapy for serious disorders including hypertension, neuropathic pain, stroke, Alzheimer's, and Parkinson's disease[3–6]. L-type calcium ($Ca_V1.1$–$1.4$) channels are inhibited by dihydropyridines (DHPs), phenylalkylamines, and benzothiazepines[7], while $Ca_V2.1$–$2.3$ channels are blocked by distinct venom toxins[8].



Correspondence: Henry M. Colecraft, Department of Physiology and Cellular Biophysics, Columbia University, College of Physicians and Surgeons, 504 Russ Berrie Pavilion, 1150 St. Nicholas Avenue, New York, NY 10032, Phone: 212-851-5372, hc2405@columbia.edu.

[*]these authors contributed equally

The authors declare no competing financial interests.

**Author Contributions**

LLH generated the plasmid constructs used in Figs. 1 and 2, designed experiments, performed electrophysiological experiments and analyses for Figs. 1 and 2; TTY performed all electrophysiological experiments and analyses for Figs. 3, 4, 5 and 6, performed some electrophysiological experiments and analyses for Fig. 2, designed experiments, made figures, and helped write the paper; MC generated the constructs used in Figs. 3, 4 and 5; KF generated the constructs used in Fig. 6; HMC obtained funding, thought of the concept, analyzed data, made figures, and wrote the paper.

Nevertheless, the full potential of calcium channel blocker (CCB) therapy remains unrealized due to a lack of selective and tissue-specific small molecule inhibitors for individual $Ca_V1/Ca_V2$ channel types. For example, clinically used L-type CCBs do not discriminate effectively among $Ca_V1.1$–$Ca_V1.4$ isoforms[9]. Because L-type channels are widely expressed, this raises significant concerns for off-target effects when targeting specific $Ca_V1$ isoforms for neurological disorders such as Alzheimer's and Parkinson's diseases[3,5]. Genetically-encoded intracellular-acting CCBs have the potential for a high therapeutic index because they can be expressed in a locally restricted manner[2,10].

RGK (Rad/Rem/Rem2/Gem/Kir) GTPases are monomeric Ras-like G-proteins that powerfully inhibit all $Ca_V1/Ca_V2$ channels[11–13]. Two proof-of-concept experiments have demonstrated the potential powerful applications of RGK proteins as genetically encoded CCBs. First, local gene delivery of Gem to the atrioventricular (AV) node slowed AV nodal conduction and reduced heart rate in a porcine atrial fibrillation model[10]. Second, targeting Rem to caveolae in single cardiomyocytes permitted selective inhibition of $Ca_V1.2$ channels in this sub-cellular compartment[14]. The ability to inhibit $Ca_V1/Ca_V2$ channels in such a locally restricted manner at the whole organ or single-cell level cannot be achieved with traditional small molecule CCBs. Ultimately, however, the potential applications of RGKs themselves as genetically-encoded CCBs are limited because they do not discriminate among $Ca_V1/Ca_V2$ isoforms, and they have other diverse binding partners and biological functions including regulating the cytoskeleton[11,15,16]. These challenges may be overcome if it were possible to exploit the mechanism of action of RGKs to derive general principles for designing novel CCBs. Here, we achieve this objective inspired by insights into how the RGK protein, Rem, inhibits $Ca_V1/Ca_V2$ channels.

## Results

### Differential tuning of $Ca_V1/Ca_V2$ channels by engineered Rem

Wild-type Rem targets to the plasma membrane using a polybasic C-terminus tail and constitutively inhibits all $Ca_V1$ and $Ca_V2$ channel isoforms. Deleting the Rem C-terminus tail ($Rem_{265}$) ablates both membrane targeting and $I_{Ca}$ inhibition. We previously discovered that fusing the C1 domain from protein kinase Cγ ($C1_{PKC}$) to $Rem_{1–265}$ enables it to be dynamically recruited to the plasma membrane with the phorbol ester, phorbol-12,13-dibutyrate (PdBu), resulting in concomitant inhibition of $I_{Ca}$. A surprising, but potentially fortuitous, feature of $Ca_V$ channel inhibition by $Rem_{265}$-$C1_{PKC}$ was that it displayed apparent selectivity, being effective for $Ca_V1.2$ and $Ca_V2.2$, but inert against $Ca_V2.1$ and $Ca_V2.3$. As a prelude to investigating whether the mechanism of Rem inhibition of $Ca_V1/Ca_V2$ channels could be exploited to develop a general method for developing genetically-encoded CCBs, we explored the possibility of tuning the selectivity and potency of PdBu-inducible Rem-based CCBs by varying the relative positioning of the $C1_{PKC}$ motif in truncated Rem (Fig. 1a). When expressed in HEK293 cells, all the truncated-Rem/$C1_{PKC}$ fusion proteins are basally cytosolic, and are rapidly recruited to the plasma membrane with PdBu (Fig. 1b, c). Under basal conditions, robust whole-cell currents were recorded from cells co-expressing distinct $Ca_V1/Ca_V2$ channel subunits ($\alpha_1$+β) and the different Rem/$C1_{PKC}$ fusion constructs, enabling their selectivity and potency to be tested by adding 1 μM

PdBu (Fig. 1d–g). Surprisingly, subtle differences in the relative position of $C1_{PKC}$ in truncated Rem dramatically impacted the comparative effectiveness of the resulting protein for $Ca_V2.1$ and $Ca_V2.2$ channels. For example, CFP-$Rem_{1–265}$-$C1_{PKC\gamma}$ inhibited $Ca_V2.2$ (and $Ca_V1.2$) channels in response to PdBu, but was ineffective on $Ca_V2.1$ (Fig. 1d, h). In sharp contrast, simply shifting the $C1_{PKC}$ motif 15 residues closer to the G-domain produced CFP-$Rem_{1–250}$-$C1_{PKC\gamma}$ which permitted PdBu-induced inhibition of $Ca_V2.1$ (and $Ca_V1.2$) but was inert against $Ca_V2.2$ (Fig. 1e, h). Similarly, whereas $C1_{PKC}$-YFP-$Rem_{1–265}$ was effective for $Ca_V2.2$ but not $Ca_V2.1$ (Fig. 1f, h), $C1_{PKC}$-$Rem_{78–265}$-CFP had the opposite preference, with selectivity for $Ca_V2.1$ over $Ca_V2.2$ (Fig. 1g, h). By contrast with the tunable selectivity for $Ca_V2.2$/$Ca_V2.1$ channels, $Ca_V1.2$ was uniformly sensitive to all four truncated-Rem/$C1_{PKC}$ constructs. Overall, these results provide the novel observation that selectivity for distinct $Ca_V2$ channels can be engineered into Rem-based CCBs simply by altering the relative positioning of the inducible membrane-anchoring domain.

## Conversion of auxiliary $Ca_V\beta_3$ into a $Ca_V$ channel inhibitor

How does Rem binding to the plasma membrane result in $Ca_V$ channel inhibition, and can this mechanism be exploited to identify a general method for developing genetically-encoded CCBs? A critical clue for these questions is that in addition to membrane targeting (Fig. 1), binding to auxiliary $Ca_V\beta$ subunits is also required for $Ca_V1.2$ channel inhibition by CFP-$Rem_{1–265}$-$C1_{PKC}$[17–19]. $Ca_V\beta$s bind the intracellular domain I-II loop of pore-forming $\alpha_1$-subunits and promote channel trafficking to the plasma membrane, as well as modulating channel activation and inactivation gating[20]. To explain the dual requirement of membrane targeting and β binding for Rem inhibition of $Ca_V1.2$ open probability ($P_o$), we hypothesized that though cytosolic variants of Rem constitutively associate with $Ca_V\beta$s in $Ca_V1$/$Ca_V2$ channel complexes, they are functionally silent, allowing the channel to gate and conduct current normally with depolarization (Fig. 2a, *top left*). By contrast, membrane-targeted Rem ‘tugs’ on $Ca_V\beta$ and by extension, the associated $\alpha_1$-subunit I–II loop, inducing a conformational change that closes the channel pore (Fig. 2a, *top right*). This allosteric model predicts it should be possible to convert the normally stimulatory $Ca_V\beta$ into a $Ca_V$ channel inhibitor by directly inducing its association with the plasma membrane (Fig. 2a, *bottom*). We tested this idea by fusing $C1_{PKC}$ directly to the C-terminus of CFP-$\beta_3$ (Fig. 2b). CFP-$\beta_3$-$C1_{PKC\gamma}$ is basally cytosolic but is rapidly recruited to the plasma (and nuclear) membrane with 1 μM PdBu (Fig. 2b, *bottom left*). When co-expressed with $Ca_V2.2$ ($\alpha_{1B}$), CFP-$\beta_3$-$C1_{PKC\gamma}$ supported robust basal $Ba^{2+}$ current ($I_{Ba}$), signifying a retained ability to promote $\alpha_1$-subunit membrane-trafficking and modulate gating (Fig. 2c). Remarkably, exposure to 1 μM PdBu resulted in a gradual decrease of $I_{Ba}$, peaking at 50% inhibition after 5 min (Fig. 2c, *middle*). The decrease in $I_{Ba}$ extended across all relevant test pulse potentials, with no shift in the current density–voltage (*I–V*) relationship (Fig. 2c, *right*). Importantly, control cells expressing $\alpha_{1B}$ + wild type (WT) β are not blocked by PdBu[18] (Supplementary Fig. S1). Therefore, directly anchoring CFP-$\beta_3$-$C1_{PKC\gamma}$ to the plasma membrane translates into $I_{Ba}$ inhibition. This conversion of a normally stimulatory $Ca_V\beta$ subunit into a CCB provides strong evidence in support of the allosteric pore-closing model we propose for membrane-targeted Rem (Fig. 2a).

$Ca_V\beta$s have a conserved core comprised of a *src* homology 3 (SH3) and guanylate kinase (GK)-like domains separated by a variable HOOK domain, and flanked by variable-length unstructured N- and C-termini[21–23]. An $\alpha_1$-binding pocket (ABP) in $Ca_V\beta$ GK binds a conserved 18-residue $\alpha_1$ interaction domain (AID) in the $\alpha_1$-subunit I-II loop[21–24]. We hypothesized that placing $C1_{PKC\gamma}$ closer to GK would result in a more potent, and possibly, kinetically faster $\beta_3$-based CCB. This is because the long and presumably floppy $Ca_V\beta$ C-terminus might be expected to introduce some slackness in the putative PdBu-induced channel conformational change (Fig. 2a). To test this idea we generated a series of constructs in which the relative distance between $C1_{PKC\gamma}$ and GK was systematically varied by serial truncations of the long, unstructured $\beta_3$ C-terminus (Fig. 2b). The most extreme case featured $C1_{PKC\gamma}$ placed immediately downstream of GK, with no intervening $\beta_3$ C-terminus sequence, generating CFP-$\beta_3[C_0]$-$C1_{PKC\gamma}$. Cells co-expressing $\alpha_{1B}$ + CFP-$\beta_3[C_0]$-$C1_{PKC\gamma}$ displayed robust basal $I_{Ba}$, and exposure to 1 μM PdBu resulted in a strong (80%), rapid-onset inhibition of current (Fig. 2d). A construct in which $C1_{PKC\gamma}$ was separated from GK by 16 residues of the C-terminus, CFP-$\beta_3[C_{16}]$-$C1_{PKC}$, displayed the deepest PdBu-induced inhibition (90% inhibition at +10 mV test potential), with kinetics of onset intermediate between CFP-$\beta_3$-$C1_{PKC\gamma}$ and CFP-$\beta_3[C_0]$-$C1_{PKC\gamma}$ (Fig. 2e). Population data from experiments using distinct variable-C-terminus-length constructs revealed a robust 60–90% PdBu-induced inhibition of $Ca_V2.2$ for $\beta_3$-CCBs with C-termini ≤ 64 residues, some of which were significantly different from the 50% inhibition seen with full-length $\beta_3$ (Fig. 2f, * $P < 0.05$ compared to CFP-$\beta_3$-$C1_{PKC\gamma}$, by one-way ANOVA and Bonferroni test, $n = 6$ for each point). Cells expressing $\alpha_{1B}$ + CFP-$\beta_3[C_{16}]$-$C1_{PKC}$ + $\alpha_2\delta$-1 were similarly inhibited by PdBu, indicating that the $\alpha_2\delta$-1 subunit does not prevent this effect (Supplementary Fig. S2). To determine whether this mechanism of inhibition could be generalized to other $Ca_V$ channels, we also assessed the efficacy of distinct $\beta_3$-CCBs on $Ca_V2.1$ and $Ca_V1.2$ channels (Fig. 2f, Supplementary Figs. S3 and S4). We found that the phenomenon was indeed evident in these other channels— for $Ca_V1.2$ the inhibition profile conferred by different $\beta_3$-CCBs was similar to $Ca_V2.2$ (Fig. 2f, *right*), whereas $Ca_V2.1$ displayed a solid but significantly different inhibition pattern from $Ca_V2.2$ (Fig. 2f, *middle*, # $P < 0.05$ compared to $Ca_V2.2$ inhibition, two-tailed unpaired *t* test, $n = 6$ for each point). Regarding the mechanism of inhibition of the $\beta_3$-CCBs, we found that PdBu markedly decreased whole-cell current without affecting gating currents (Supplementary Fig. S5). This suggests a selective reduction in either channel $P_o$ or single channel conductance with no change in the number of channels at the cell surface, similar to what we previously found for PdBu-induced Rem-based CCBs[18].

The effectiveness of membrane-targeted $\beta_3$-CCBs in blocking $Ca_V1/Ca_V2$ channels was surprising given that two $Ca_V\beta$ isoforms, $\beta_{2a}$ and $\beta_{2e}$, natively localize to the plasma membrane via their N-termini but, nevertheless, yield robust $I_{Ba}$ when reconstituted with $\alpha_1$-subunits[25,26]. Moreover, artificially introducing membrane-targeting domains to N-termini of cytosolic $Ca_V\beta$s does not compromise their ability to reconstitute functional channels with $\alpha_1$-subunits[27,28]. One possibility for the discrepancy is that the polarity of the membrane targeting domain on $Ca_V\beta$ is important for the impact on channel gating. We examined this idea by placing $C1_{PKC\gamma}$ on $Ca_V\beta_3$ N-terminus and testing its effectiveness as a CCB. $C1_{PKC}$-$\beta_3$-CFP reconstituted robust $I_{Ba}$ when co-expressed with $Ca_V2.2\alpha_{1B}$, but

exposure to PdBu had minimal impact on $I_{Ba}$ (Supplementary Fig. S6), suggesting polarity of the membrane-targeting domain is important for β-CCB efficacy.

## General method for converting $\alpha_1$-binding proteins into CCBs

The $\beta_3$-CCB results are consistent with a model in which membrane-targeted Rem uses $Ca_V\beta$ as a "handle" to alter the conformation of $\alpha_1$-subunit I–II loop in a manner that closes the channel pore. Since intracellular loops and termini of $Ca_V1/Ca_V2$ channels (Fig. 3a) engage in numerous protein-protein interactions, both common and unique, we speculated that other $\alpha_1$-binding proteins might be similarly used as 'handles' to manipulate channel gating. If so, this would reveal a generalized principle for designing novel genetically-encoded CCBs. To test this premise, we focused on three different proteins (14-3-3, $Ca^{2+}$-calmodulin-dependent protein kinase II, and calmodulin) known to bind intracellular domains of individual $Ca_V1/Ca_V2$ channels[29–34]. Wild-type 14-3-3ε binds $Ca_V2.2\alpha_{1B}$ C-terminus and modulates channel inactivation properties[31]. To determine whether 14-3-3 could be converted into a small-molecule-regulated $Ca_V2.2$ inhibitor, we generated $C1_{PKC\gamma}$-mCherry-14-3-3ε, which is normally cytosolic but rapidly translocates to the plasma membrane with PdBu (Fig. 3b). Cells co-expressing $Ca_V2.2$ ($\alpha_{1B}$ + β) and $C1_{PKC}$-mCherry-14-3-3 displayed robust basal $I_{Ba}$, and exposure to 1 μM PdBu caused a rapid 60% inhibition of $I_{Ca}$ amplitude (Fig. 3c). Similar results were obtained with $Ca_V2.1$ and $Ca_V1.2$, respectively, indicating that these channels also interact with 14-3-3ε (Fig. 3c). To our knowledge, it was not previously known that $Ca_V1.2$ bound 14-3-3 proteins. Replacing $C1_{PKC\gamma}$ with an 18-residue palmitoylated membrane-targeting peptide (mem) from neuromodulin generated mem-mCherry-14-3-3ε which constitutively targeted to the plasma membrane (Fig. 3d). Remarkably, mem-mCherry-14-3-3ε resulted in strong constitutive inhibition of $Ca_V2.2$, $Ca_V2.1$, and $Ca_V1.2$ channels across all test voltages (Fig. 3e). Control cells expressing mCherry-14-3-3 with $Ca_V2.2$ displayed neither inducible nor constitutive $I_{Ba}$ inhibition (Supplementary Fig. S1).

We next considered whether we could convert $Ca^{2+}$-calmodulin-dependent protein kinase II (CaMKII) into a CCB. CaMKII has been found to constitutively bind $Ca_V1.2$[29] and $Ca_V2.1$[30] channels, respectively. CaMKII bound to $Ca_V1.2$ C-terminus was found necessary for $Ca^{2+}$-dependent facilitation of $I_{Ca,}$[29]. Further, CaMKII binding to $Ca_V2.1$ C-terminus slows channel inactivation kinetics and regulates short-term synaptic plasticity in neurons[30]. CaMKII holo-enzyme is a multimer of 12 monomeric subunits[35]. Each monomer (475 amino acids) has three distinct domains: an N-terminal catalytic domain (residues 1–274) that mediates kinase activity, a central regulatory domain (residues 275–314) that exerts basal auto-inhibitory control of the kinase domain, and an association domain (residues 315–475) that mediates subunit assembly. The catalytic domain of CaMKII mediates binding to $Ca_V1.2$ channels[29]. To assess the possibility of converting CaMKII into a CCB we fused either $C1_{PKC\gamma}$ or the polybasic membrane-targeting tail from K-Ras to the C-terminus of CaMKII catalytic domain (residues 1–274). We also introduced a K42M point mutation that renders the kinase catalytically dead[35]. $CaMKII_{[1–274,K42M]}$-$C1_{PKC}$ inducibly translocated to the membrane (Fig. 3f) and inhibited $Ca_V2.2$ and $Ca_V1.2$ channels in response to PdBu (Fig. 3g). Surprisingly, $Ca_V2.1$ channels were not inhibited by membrane-translocated $CaMKII_{[1–274,K42M]}$-$C1_{PKC}$ (Fig. 3g, *middle*). By contrast, $CaMKII_{[1–274,K42M]}$-$KRas_{tail}$

was constitutively associated with the plasma membrane (Fig. 3h), and caused a deep inhibition of all three $Ca_V$ channels (Fig. 3i). Beyond providing an additional proof of the principle for generating novel genetically-encoded CCBs, these results suggest that recombinant $Ca_V2.2$ channels may also bind CaMKII. The discrepancy in $Ca_V2.1$ sensitivity to $CaMKII_{[1–274,K42M]}$-$C1_{PKC}$ and $CaMKII_{[1–274,K42M]}$-$KRas_{tail}$ suggests that inhibition by the CaMKII-based inhibitor in this channel may be kinetically slow such that it is only apparent with the constitutive CCB.

Finally, we explored the feasibility of using CaM to create a genetically-encoded CCB. CaM is known to bind $Ca_V1$ and $Ca_V2$ channels and mediates their regulation by $Ca^{2+}$ ions. We generated mCherry-CaM-$C1_{PKC}$ which displayed basal cytosolic localization but was translocated to the plasma membrane with PdBu (Fig. 4a). Because the endogenous CaM concentration is relatively high, the efficacy of CaM based CCBs would be expected to depend critically on how effectively they displace endogenous CaM from the channels. We used $Ca^{2+}$-dependent inactivation (CDI) of $Ca_V1.2$ channels as a biosensor to gain insights into how effectively $C1_{PKC}$-tagged wt and mutant CaM displaced endogenous CaM. When co-expressed with mCherry-CaM-$C1_{PKC}$, recombinant $Ca_V1.2$ channels ($\alpha_{1C} + \beta_{2a}$) displayed $Ba^{2+}$ currents that showed a slow monotonic voltage-dependent inactivation (Fig. 4b). With $Ca^{2+}$ as charge carrier, the same channels exhibited a fast and deep decrease in current amplitude with the kinetic signature of CDI (Fig. 4b). When co-expressed with a mutant mCherry-$CaM_{1234}$-$C1_{PKC}$ in which with all four EF hands mutated so they no longer bind $Ca^{2+}$, $Ca_V1.2$ channels displayed $Ca^{2+}$ currents in which CDI was virtually eliminated (Fig. 4b). This result indicates that the over-expressed mCherry-$CaM_{1234}$-$C1_{PKC}$ effectively out-competes endogenous CaM for binding to $Ca_V1.2$, and further demonstrates that the tags do not interfere with CaM binding to $Ca_V$ channels. We found $Ca_V2.2$ channels co-expressed with mCherry-$CaM_{1234}$-$C1_{PKC}$ were rapidly inhibited by PdBu (Fig. 4c). Surprisingly, both $Ca_V2.1$ and $Ca_V1.2$ co-expressed with mCherry-$CaM_{1234}$-$C1_{PKC}$ were unaffected by PdBu (Fig. 4c). Because CaM binds to all three channels[32,33,36,37], these results suggest that the mere existence of a binding site for a cytosolic protein on the channel may not be sufficient to generate an inducible CCB in all cases. Another possibility is that potential inhibition of $Ca_V2.1$ and $Ca_V1.2$ induced by membrane-targeting mCherry-$CaM_{1234}$-$C1_{PKC}$ is kinetically slow such that it does not occur during the 5–10 min time course of our electrophysiological assay.

Overall, these data demonstrate diverse intracellular proteins interacting with $Ca_V1/Ca_V2$ channels can be converted into constitutive or inducible CCBs with distinctive potency and/or selectivity. We have termed this general method Channel Inactivation induced by Membrane-tethering of an associated Protein (ChIMP). The acronym is apropos given the imagery of closing a channel pore by the induced ‘swinging’ of an associated protein from the cytoplasm to the plasma membrane (Fig. 2a).

### Effectiveness of 14-3-3-based CCB on native $Ca_V$ channels

The results to this point have tested the efficacy of genetically-encoded CCBs on recombinant $Ca_V$ channels reconstituted in HEK 293 cells. Because native $Ca_V$ channels are typically associated with macromolecular complexes and have a more complicated nano-

enviroment than recombinant channels in heterologous cells, it was important to verify that the genetically-engineered CCBs were effective against native $Ca_V$ channels. We first examined the impact of mem-mCherry-14-3-3ε on $Ca_V$ channels recorded from primary cultures of murine dorsal root ganglion (DRG) neurons. DRG neurons express multiple $Ca_V1/Ca_V2$ channel currents[38]. We used adenoviral vectors to express either mCherry-14-3-3 or mem-mCherry-14-3-3 (Fig. 5a) in cultured DRG neurons. Cells expressing mCherry-14-3-3 displayed an *I–V* relationship that was indistinguishable from that obtained with control uninfected neurons (Fig. 5b, *left;* $I_{peak}$ at 0 mV = 57.2 ± 9.9 pA/pF, $n$ = 6 for control neurons, $I_{peak}$ = 62.0 ± 19.6 pA/pF, $n$ = 6 for mCherry-14-3-3-expressing neurons). By contrast, expression of mem-mCherry-14-3-3ε in DRG neurons markedly suppressed endogenous $I_{Ba}$ within 24 hrs of adenoviral infection (Fig. 5b, *right;* $I_{peak}$ = 6.3 ± 1.5 pA/pF, $n$ = 6 for mem-mCherry-14-3-3-expressing neurons, $P < 0.05$ compared to control using unpaired *t* test). We obtained similar results for nerve growth factor (NGF) differentiated rat pheochromocytoma (PC-12) cells (Fig. 5c) which contain $Ca_V2.2$ and $Ca_V1.2$ channels that trigger exocytosis[39]. These results demonstrate that genetically-engineered CCBs developed according to the ChIMP principle are also effective against native $Ca_V1/Ca_V2$ channels despite their more elaborate nano-environment.

## Potential use of ChIMP to discover small molecule CCBs

The results so far suggest the general principle that the discovery process for new CCBs may be decomposed into two parts: firstly, finding a molecule that binds an appropriate $\alpha_1$-subunit cytoplasmic region (a ‘handle’), and secondly, a transduction step involving the anchoring of the ‘handle’ molecule to the plasma membrane. We next considered two ancillary issues. First, whether the ‘handle’ could be a small molecule rather than a protein as we have so far demonstrated. If so, the ChIMP method could potentially be extended to small-molecule drug discovery. Second, whether it would be possible to develop a method to systematically identify which areas in $\alpha_1$ cytoplasmic regions are appropriate target binding-sites that are permissive for regulated closure of the channel pore. To concurrently address these two issues, we adapted a heterodimerization strategy which relies on the ability of the small molecule rapamycin to simultaneously bind two proteins, FK506-binding protein (FKBP) and a fragment of the mammalian target of rapamycin (FRB), respectively[40]. We inserted FKBP (one insert per channel) at four different positions within $Ca_V1.2$ $\alpha_{1C}$ subunit intracellular regions (N-terminus, I-II loop, and at proximal and distal positions in the C-terminus) (Fig. 6a). All these constructs expressed currents when co-expressed with $\beta_{2a}$ and a constitutively membrane-targeted FRB (LDR) in HEK 293 cells[18,41]. 1μM rapamycin caused a rapid inhibition of $I_{Ba}$ in channels with FKBP inserted into the C-terminus (Fig. 6d, e). By contrast, channels with FKBP inserted at the N-terminus and in the distal I–II loop, respectively, did not display rapamycin-induced decrease in current (Fig. 6b, c). Neither of the two C-terminus FKBP-fused channels responded to rapamycin in the absence of LDR (Supplementary Fig. S7). These findings offer a critical proof-of-concept that the ChIMP approach can potentially be used to discover new CCBs by using high throughput screening to find molecules that bind appropriate ‘handle sites’ in $Ca_V$ $\alpha_1$-subunits, and conjugating them to a membrane-targeting module. A major challenge that would need to be overcome to realize this possibility is developing sensitive high throughput screens to identify small molecules that bind intracellular domains of $Ca_V$

channels. One possibility is to use purified tagged $Ca_V$ $\alpha_1$ intracellular loops to probe small molecule microarrays[42,43].

## Discussion

In this work we report the discovery that diverse proteins/molecules that bind distinct sites in intracellular loops of $Ca_V1/Ca_V2$ channels can be used as 'handles' to inhibit $I_{Ca}$ through their controlled anchoring to the plasma membrane. This new insight paves the way for developing customized CCBs with selectivity for distinct $Ca_V1/Ca_V2$ channels based on the identity of the pore-forming $\alpha_1$-subunit, the auxiliary $Ca_V\beta$, or other associated cytoplasmic proteins. Genetically-encoded CCBs are potentially desirable because they can be expressed in a geographically restricted fashion thereby eliminating off-target effects that may confound small-molecule drug therapy[2,10]. Furthermore, genetically-encoded CCBs can be engineered to block molecularly identical $Ca_V$ channels with sub-cellular specificity. For example, a caveolae-targeted Rem has been shown to selectively inhibit caveolae-localized $Ca_V1.2$ channels in heart cells while sparing dyadic $Ca_V1.2$ channels that trigger muscle contraction[14]. Because caveolae-localized $Ca_V1.2$ channels are hypothesized to selectively signal to pathological cardiac hypertrophy, it is proposed that caveolae-specific $Ca_V1.2$ channel inhibitors could be an effective therapy for adverse remodeling of the heart[14]. RGK proteins have so far been used in proof-of-concept experiments to demonstrate the utility of genetically-encoded CCBs[10,14]. However, the potential clinical use of RGKs is complicated by their broad biological effects, diverse binding partners, and lack of specificity and controllability[11]. This work introduces ChIMP as a generalized method for developing novel genetically-encoded CCBs with distinct potency, selectivity, and kinetics. A caveat for the work is that the CCBs we have generated so far are derived from naturally occurring proteins that also have their own specific functions and binding partners in cells. Nevertheless, the general insights obtained from developing these proteins can now be potentially coupled with new technologies for evolving protein molecules that bind to target sites with high specificity, such as DARPins[44] and intrabodies[45], to develop highly selective $Ca_V1/Ca_V2$ channel blockers. Another aspect of the ChIMP technology that can be greatly improved relates to the method for inducing membrane targeting of the 'handle' protein. Here, we used PdBu and rapamycin-mediated heterodimerization as convenient tools to demonstrate proof-of-concept of the ChiMP method. However, PdBu activates endogenous protein kinase C, and rapamycin associates with endogenous FKBP and mammalian target of rapamycin (mTOR), a protein kinase involved in cell proliferation, growth, and survival. Hence, these two agents may be inappropriate for potential *in vivo* applications. Recently, several genetically encoded dimerizers based on plant photoreceptors that permit light-regulated, reversible protein heterodimerization have been developed[46–48]. Marriage of light-regulated heterodimerization with ChIMP could provide a powerful general method for optogenetic control of $Ca_V$ channels and is an exciting prospect for future experiments.

We previously reported that Rem which normally constitutively targets to the plasma membrane and inhibits $Ca_V$ channels could be converted into a small-molecule-regulated inducible CCB by dynamically regulating its association with the plasma membrane[18,19]. However, it was unknown how targeting Rem to the membrane caused $Ca_V$ channel inhibition. This work supports a model where membrane-targeted Rem uses $Ca_V\beta$ as a

bridge to alter the conformation of the I-II loop in a manner that closes the channel. This is an important new insight into the mechanism of action of RGKs, particularly in light of data that have raised questions about a role for RGK binding to $Ca_V\beta$ in the mechanism for $Ca_V$ channel inhibition[49]. More generally, regulation of channel gating by induced conformational changes in intracellular domains is a rather common phenomenon that occurs in many different ion channels. For example, cyclic nucleotides and $Ca^{2+}$ control the opening of cyclic nucleotide gated (CNG) and large conductance $K^+$ (BK) channels, respectively, by binding to channel intracellular domains[50,51]. Moreover, engagement of cytoplamic domains with the plasma membrane through interaction with phosphoinositide lipids regulates the gating of ion channels such as the inward rectifier $K^+$ channel Kir2.2[52] and TRPV1[53]. From this perspective, the ChIMP approach could provide important insights into how distinct intracellular domains link to channel gating in different ion channels.

The major conceptual advance in this study is that diverse cytosolic proteins or small molecules that bind distinct sites in intracellular loops of $Ca_V1/Ca_V2$ channels can likewise be converted to constitutive or inducible $Ca_V$ channel inhibitors according to the mode of their anchoring to the plasma membrane. This is a non-trivial advance because it suggests a general method for developing novel genetically encoded blockers for many ion channel types. Ion channels are ubiquitous and essential to the biology of all cell types, and their dysfunction underlies many human diseases[54]. Selective ion channel modulators are highly sought after as therapeutics and research tools. However, there is a lack of specific modulators for many ion channel species. The ChIMP strategy may potentially be applied to develop novel blockers for a broad cohort of ion channels.

A corollary benefit of the ChIMP approach is its potential to provide a robust functional readout as to whether individual proteins directly interact with intracellular domains of recombinant $Ca_V1/Ca_V2$ channels. In our study, we discovered for the first time that recombinant $Ca_V1.2$ binds 14-3-3 and that $Ca_V2.2$ binds CaMKII. A proteomic study of the $Ca_V2$ channel nano-environment in mammalian brain indicates these channels are associated with a protein network gathered from a pool of ~200 proteins with distinct abundance and preference for $Ca_V2.1$-$Ca_V2.3$ subtypes[55]. Our studies suggest how $Ca_V1/Ca_V2$ channels may be used as a biosensor to validate some of these putative protein interactions.

## Methods

### cDNA cloning

To generate fluorescent-protein-tagged constructs, cyan or yellow fluorescent protein (CFP or YFP) was amplified using polymerase chain reaction (PCR) and cloned into pcDNA4.1 (Invitrogen) using *Kpn*I and *BamH*I sites. CFP–$Rem_{1–265}$–$C1_{PKC\gamma}$ and CFP–$Rem_{1–250}$–$C1_{PKC\gamma}$ were generated by using overlap extension PCR to fuse residues 26–89 of mouse PKCγ to the C-terminus of $Rem_{1–265}$ and $Rem_{1–250}$, respectively. The fusion product was subsequently cloned downstream of CFP using *BamH*I and *EcoR*I sites. To create $C1_{PKC\gamma}$-$Rem_{78–265}$–CFP, $C1_{PKC\gamma}$ was cloned into pcDNA4.1 (Invitrogen) using *Kpn*I and *BamH*I sites. $Rem_{78–265}$ and CFP were subsequently amplified and cloned downstream of $C1_{PKC\gamma}$ using *BamH*I/*EcoR*I and *EcoR*I/*Xba*I sites, respectively. $C1_{PKC\gamma}$-YFP-$Rem_{1–265}$ was produced by first using overlap extension PCR to fuse $C1_{PKC\gamma}$ to the N terminus of YFP.

The resulting fusion product was cloned upstream of $Rem_{1–265}$ using *Kpn*I and *BamH*I sites. CFP-$\beta_3$-$C1_{PKC\gamma}$ was generated by using overlap extension PCR to fuse $C1_{PKC\gamma}$ to the C terminus of $\beta_3$. The fusion product was then cloned downstream of CFP using *BamH*I and *EcoR*I sites. To generate $C1_{PKC\gamma}$-mcherry-14-3-3, we used overlap extension PCR to fuse $C1_{PKC\gamma}$ to the N terminus of mCherry. The fusion product was cloned into pcDNA4.1 (Invitrogen) using *Kpn*I and *BamH*I sites. 14-3-3 was PCR amplified and cloned downstream of mcherry using *BamH*I and *Xho*I sites. To create mcherry-$CaMKII_{1–274K42M}$-$C1_{PKC\gamma}$, we used overlap extension PCR to fuse $C1_{PKC\gamma}$ to the C terminus of $CaMKII_{1–274}$. The fusion product was cloned into pcDNA4.1 (Invitrogen) using *BamH*I and *Xho*I sites sites. mcherry was PCR amplified and cloned upstream using *Kpn*I and *BamH*I sites. Point mutation in mcherry-$CaMKII_{1–274K42M}$-$C1_{PKC\gamma}$ was introduced using the QuikChange Site-Directed Mutagenesis Kit (Stratagene). To generate FKBP-fused $\alpha_{1C}$ constructs, we used overlap extension PCR to fuse YFP to the C terminus of $\alpha_{1C}$. The fusion product was cloned into pcDNA3.1 (Invitrogen) using *Kpn*I and *Xba*I sites. FKBP was inserted into distinct regions of $\alpha_{1C}$ intracellular loops using In-fusion Cloning Kit (Clontech). All PCR products were verified by sequencing.

## Cell culture and transfection

Low-passage-number HEK 293 cells were maintained in DMEM supplemented with 10% FBS and 100 μg $ml^{-1}$ penicillin-streptomycin. For electrophysiology and flow cytometry experiments, HEK 293 cells cultured in 6–cm tissue culture dishes were transiently transfected with $Ca_V1/Ca_V2$ $\alpha_1$ (6 μg), $\beta_3$ (6 μg), T antigen (2 μg), and the appropriate GEMIICC construct (4 μg), using the calcium phosphate precipitation method. Cells were washed with PBS 5–8 h after transfection and maintained in supplemented DMEM. For confocal microscopy experiments, transfected HEK 293 cells were replated onto fibronectin-coated culture dishes with No. 0 glass coverslip bottoms (MaTek). For electrophysiology experiments cells were replated onto fibronectin-coated glass coverslips 24 h after transfection.

DRG neurons were maintained in 96.5ml Neurobasal A medium supplemented with 2ml B-27, 100 μg $ml^{-1}$ Pen/strep, 0.5 ml L-glutamine, 50 ng $ml^{-1}$ NGF, 2 ng $ml^{-1}$ GDNF, and 10 μM Ara-C. For electrophysiology experiments, DRG neurons cultured in 2–cm tissue culture dishes were infected with the appropriate adenovirus. Undifferentiated PC12 cells were maintained in RPMI supplemented with 10% horse serum, 5% FBS and 100 μg $ml^{-1}$ penicillin-streptomycin. Differentiated PC12 cells were maintained in RPMI supplemented with 1% horse serum. 50 ng $ml^{-1}$ NGF was added to media just prior to use. For electrophysiology experiments, PC12 cells cultured in 6–cm tissue culture dishes were infected with the appropriate adenovirus.

## Electrophysiology

Whole-cell recordings of HEK cells were conducted 48–72 h after transfection using an EPC–8 or EPC–10 patch clamp amplifier (HEKA Electronics) controlled by PULSE software (HEKA). Micropipettes were fashioned from 1.5–mm thin-walled glass with filament (WPI Instruments) and filled with internal solution containing (in mM): 135 cesium methanesulphonate ($MeSO_3$), 5 CsCl, 5 EGTA, 1 $MgCl_2$, 4 MgATP (added fresh) and 10

HEPES (pH 7.3). Series resistance was typically between 1.5–2 MΩ. There was no electronic series resistance compensation. External solution contained (in mM): 140 tetraethylammonium–$MeSO_3$, 5 $BaCl_2$, and 10 HEPES (pH 7.3). Whole-cell *I–V* curves were generated from a family of step depolarizations (−40 to +100 mV from a holding potential of −90 mV). Currents were sampled at 25 kHz and filtered at 5 or 10 kHz. Traces were acquired at a repetition interval of 6 s. Leak and capacitive currents were subtracted using a P/8 protocol.

Whole-cell recordings of DRG and PC12 cells were conducted 24–48 h after infection. HEK cell internal solution was used for both DRG and PC12 cells. HEK cell external solution was used for PC12 cells. HEK cell external solution with 0.5 μM TTX was used for DRG neurons.

### Confocal microscopy

Static images of CFP–$Rem_{1–265}$-$C1_{PKC\gamma}$, CFP-β3 -$C1_{PKC\gamma}$, and mcherry-$C1_{PKC\gamma}$-14-3-3 constructs were observed using a Leica TCS SPL AOBS MP Confocal microscope system and a 40X oil objective (HCX PL APO 1.25–.75 NA). HEK 293 cells expressing CFP, YFP, and mCherry fusion proteins were imaged using the 458, 514 and 543-nm Argon laser line, respectively, for excitation.

### Data and statistical analyses

Data were analyzed off-line using PulseFit (HEKA), Microsoft Excel and Origin software. Statistical analyses were performed in Origin using built-in functions. Statistically significant differences between means ($P < 0.05$) were determined using Student's *t* test for comparisons between two groups, or one-way ANOVA followed by pairwise means comparisons using Bonferroni test for multiple groups. Data are presented as means ± s.e.m.

## Supplementary Material

Refer to Web version on PubMed Central for supplementary material.

## Acknowledgments

The authors thank T. Meyer and T. Inoue (Stanford University) for FRB construct (LDR), Drs. Ademuyiwa Aromolaran and Prakash Subramanyam for comments on the manuscript, Dr. David Yue (Johns Hopkins University) for discussions, Drs. Llloyd Greene and Oren Levy (Columbia University) for PC12 cells, Dr. Joachim Scholz (Columbia University) for DRG neurons, and Brian Soda for assistance with the ChIMP illustration artwork. This work was supported by NIH grants RO1 HL084332 and RO1 HL069911 (to H.M.C). L.L.H was supported by a NIH postdoctoral training grant (T32 HL087745). H.M.C. is an Established Investigator of the American Heart Association.

## References

1. Catterall WA. Structure and regulation of voltage-gated Ca2+ channels. Annu Rev Cell Dev Biol. 2000; 16:521–555. [PubMed: 11031246]
2. Xu X, Colecraft HM. Engineering proteins for custom inhibition of Ca(V) channels. Physiology (Bethesda). 2009; 24:210–218. [PubMed: 19675352]
3. Anekonda TS, Quinn JF. Calcium channel blocking as a therapeutic strategy for Alzheimer's disease: the case for isradipine. Biochim Biophys Acta. 2011; 1812:1584–1590. [PubMed: 21925266]

4. Kochegarov AA. Pharmacological modulators of voltage-gated calcium channels and their therapeutical application. Cell Calcium. 2003; 33:145–162. [PubMed: 12600802]
5. Simuni T, et al. Tolerability of isradipine in early Parkinson's disease: a pilot dose escalation study. Mov Disord. 2010; 25:2863–2866. [PubMed: 20818667]
6. Triggle DJ. Calcium channel antagonists: clinical uses--past, present and future. Biochem Pharmacol. 2007; 74:1–9. [PubMed: 17276408]
7. Striessnig J, et al. Structural basis of drug binding to L Ca2+ channels. Trends Pharmacol Sci. 1998; 19:108–115. [PubMed: 9584627]
8. Uchitel OD. Toxins affecting calcium channels in neurons. Toxicon. 1997; 35:1161–1191. [PubMed: 9278968]
9. Zuccotti A, et al. Structural and functional differences between L-type calcium channels: crucial issues for future selective targeting. Trends Pharmacol Sci. 2011; 32:366–375. [PubMed: 21450352]
10. Murata M, Cingolani E, McDonald AD, Donahue JK, Marban E. Creation of a genetic calcium channel blocker by targeted gem gene transfer in the heart. Circ Res. 2004; 95:398–405. [PubMed: 15242970]
11. Yang T, Colecraft HM. Regulation of voltage-dependent calcium channels by RGK proteins. Biochim Biophys Acta. 2012; 1828:1644–1654. [PubMed: 23063948]
12. Beguin P, et al. Regulation of Ca2+ channel expression at the cell surface by the small G-protein kir/Gem. Nature. 2001; 411:701–706. [PubMed: 11395774]
13. Finlin BS, Crump SM, Satin J, Andres DA. Regulation of voltage-gated calcium channel activity by the Rem and Rad GTPases. Proc Natl Acad Sci U S A. 2003; 100:14469–14474. [PubMed: 14623965]
14. Makarewich CA, et al. A caveolae-targeted L-type Ca(2)+ channel antagonist inhibits hypertrophic signaling without reducing cardiac contractility. Circ Res. 2012; 110:669–674. [PubMed: 22302787]
15. Correll RN, Pang C, Niedowicz DM, Finlin BS, Andres DA. The RGK family of GTP-binding proteins: regulators of voltage-dependent calcium channels and cytoskeleton remodeling. Cell Signal. 2008; 20:292–300. [PubMed: 18042346]
16. Flynn R, Zamponi GW. Regulation of calcium channels by RGK proteins. Channels (Austin). 2010; 4:434–439. [PubMed: 20953143]
17. Yang T, Puckerin A, Colecraft HM. Distinct RGK GTPases Differentially Use alpha(1)- and Auxiliary beta-Binding-Dependent Mechanisms to Inhibit Ca(V)1.2/Ca(V)2.2 Channels. PLoS One. 2012; 7:e37079. [PubMed: 22590648]
18. Yang T, Suhail Y, Dalton S, Kernan T, Colecraft HM. Genetically encoded molecules for inducibly inactivating CaV channels. Nat Chem Biol. 2007; 3:795–804. [PubMed: 17952065]
19. Yang T, Xu X, Kernan T, Wu V, Colecraft HM. Rem, a member of the RGK GTPases, inhibits recombinant CaV1.2 channels using multiple mechanisms that require distinct conformations of the GTPase. J Physiol. 2010; 588:1665–1681. [PubMed: 20308247]
20. Buraei Z, Yang J. The {beta} Subunit of Voltage-Gated Ca2+ Channels. Physiol Rev. 2010; 90:1461–1506. [PubMed: 20959621]
21. Chen YH, et al. Structural basis of the alpha1-beta subunit interaction of voltage-gated Ca2+ channels. Nature. 2004; 429:675–680. [PubMed: 15170217]
22. Opatowsky Y, Chen CC, Campbell KP, Hirsch JA. Structural analysis of the voltage-dependent calcium channel beta subunit functional core and its complex with the alpha 1 interaction domain. Neuron. 2004; 42:387–399. [PubMed: 15134636]
23. Van Petegem F, Clark KA, Chatelain FC, Minor DL Jr. Structure of a complex between a voltage-gated calcium channel beta-subunit and an alpha-subunit domain. Nature. 2004; 429:671–675. [PubMed: 15141227]
24. Pragnell M, et al. Calcium channel beta-subunit binds to a conserved motif in the I-II cytoplasmic linker of the alpha 1-subunit. Nature. 1994; 368:67–70. [PubMed: 7509046]
25. Takahashi SX, Mittman S, Colecraft HM. Distinctive modulatory effects of five human auxiliary beta 2 subunit splice variants on L-type calcium channel gating. Biophys J. 2003; 84:3007–3021. [PubMed: 12719232]

26. Chien AJ, et al. Roles of a membrane-localized beta subunit in the formation and targeting of functional L-type Ca2+ channels. J Biol Chem. 1995; 270:30036–30044. [PubMed: 8530407]
27. Restituito S, et al. The [beta]2a subunit is a molecular groom for the Ca2+ channel inactivation gate. J Neurosci. 2000; 20:9046–9052. [PubMed: 11124981]
28. Suh BC, Kim DI, Falkenburger BH, Hille B. Membrane-localized beta-subunits alter the PIP2 regulation of high-voltage activated Ca2+ channels. Proc Natl Acad Sci U S A. 2012; 109:3161–3166. [PubMed: 22308488]
29. Hudmon A, et al. CaMKII tethers to L-type Ca2+ channels, establishing a local and dedicated integrator of Ca2+ signals for facilitation. J Cell Biol. 2005; 171:537–547. [PubMed: 16275756]
30. Jiang X, et al. Modulation of CaV2.1 channels by Ca2+/calmodulin-dependent protein kinase II bound to the C-terminal domain. Proc Natl Acad Sci U S A. 2008; 105:341–346. [PubMed: 18162541]
31. Li Y, Wu Y, Zhou Y. Modulation of inactivation properties of CaV2.2 channels by 14-3-3 proteins. Neuron. 2006; 51:755–771. [PubMed: 16982421]
32. Peterson BZ, DeMaria CD, Adelman JP, Yue DT. Calmodulin is the Ca2+ sensor for Ca2+-dependent inactivation of L-type calcium channels. Neuron. 1999; 22:549–558. [PubMed: 10197534]
33. Lee A, et al. Ca2+/calmodulin binds to and modulates P/Q-type calcium channels. Nature. 1999; 399:155–159. [PubMed: 10335845]
34. Zuhlke RD, Pitt GS, Deisseroth K, Tsien RW, Reuter H. Calmodulin supports both inactivation and facilitation of L-type calcium channels. Nature. 1999; 399:159–162. [PubMed: 10335846]
35. Chao LH, et al. A mechanism for tunable autoinhibition in the structure of a human Ca2+/calmodulin- dependent kinase II holoenzyme. Cell. 2011; 146:732–745. [PubMed: 21884935]
36. Liang H, et al. Unified mechanisms of Ca2+ regulation across the Ca2+ channel family. Neuron. 2003; 39:951–960. [PubMed: 12971895]
37. Van Petegem F, Chatelain FC, Minor DL Jr. Insights into voltage-gated calcium channel regulation from the structure of the CaV1.2 IQ domain-Ca2+/calmodulin complex. Nat Struct Mol Biol. 2005; 12:1108–1115. [PubMed: 16299511]
38. Scroggs RS, Fox AP. Multiple Ca2+ currents elicited by action potential waveforms in acutely isolated adult rat dorsal root ganglion neurons. J Neurosci. 1992; 12:1789–1801. [PubMed: 1578270]
39. Taylor SC, Peers C. Store-operated Ca2+ influx and voltage-gated Ca2+ channels coupled to exocytosis in pheochromocytoma (PC12) cells. J Neurochem. 1999; 73:874–880. [PubMed: 10428087]
40. Crabtree GR, Schreiber SL. Three-part inventions: intracellular signaling and induced proximity. Trends Biochem Sci. 1996; 21:418–422. [PubMed: 8987395]
41. Inoue T, Heo WD, Grimley JS, Wandless TJ, Meyer T. An inducible translocation strategy to rapidly activate and inhibit small GTPase signaling pathways. Nat Methods. 2005; 2:415–418. [PubMed: 15908919]
42. Bradner JE, et al. A robust small-molecule microarray platform for screening cell lysates. Chem Biol. 2006; 13:493–504. [PubMed: 16720270]
43. Noblin DJ, et al. A HaloTag-based small molecule microarray screening methodology with increased sensitivity and multiplex capabilities. ACS Chem Biol. 2012; 7:2055–2063. [PubMed: 23013033]
44. Boersma YL, Pluckthun A. DARPins and other repeat protein scaffolds: advances in engineering and applications. Curr Opin Biotechnol. 2011; 22:849–857. [PubMed: 21715155]
45. Zhou C, Przedborski S. Intrabody and Parkinson's disease. Biochim Biophys Acta. 2009; 1792:634–642. [PubMed: 18834937]
46. Kennedy MJ, et al. Rapid blue-light-mediated induction of protein interactions in living cells. Nat Methods. 2010; 7:973–975. [PubMed: 21037589]
47. Levskaya A, Weiner OD, Lim WA, Voigt CA. Spatiotemporal control of cell signalling using a light-switchable protein interaction. Nature. 2009; 461:997–1001. [PubMed: 19749742]

48. Yazawa M, Sadaghiani AM, Hsueh B, Dolmetsch RE. Induction of protein-protein interactions in live cells using light. Nat Biotechnol. 2009; 27:941–945. [PubMed: 19801976]
49. Fan M, Buraei Z, Luo HR, Levenson-Palmer R, Yang J. Direct inhibition of P/Q-type voltage-gated Ca2+ channels by Gem does not require a direct Gem/Cavbeta interaction. Proc Natl Acad Sci U S A. 2010; 107:14887–14892. [PubMed: 20679232]
50. Craven KB, Zagotta WN. CNG and HCN channels: two peas, one pod. Annu Rev Physiol. 2006; 68:375–401. [PubMed: 16460277]
51. Salkoff L, Butler A, Ferreira G, Santi C, Wei A. High-conductance potassium channels of the SLO family. Nat Rev Neurosci. 2006; 7:921–931. [PubMed: 17115074]
52. Hansen SB, Tao X, MacKinnon R. Structural basis of PIP2 activation of the classical inward rectifier K+ channel Kir2.2. Nature. 2011; 477:495–498. [PubMed: 21874019]
53. Cao E, Cordero-Morales JF, Liu B, Qin F, Julius D. TRPV1 channels are intrinsically heat sensitive and negatively regulated by phosphoinositide lipids. Neuron. 2013; 77:667–679. [PubMed: 23439120]
54. Ashcroft, FM. Ion Channels and Disease. Academic Press; London: 1999.
55. Muller CS, et al. Quantitative proteomics of the Cav2 channel nano-environments in the mammalian brain. Proc Natl Acad Sci U S A. 2010; 107:14950–14957. [PubMed: 20668236]

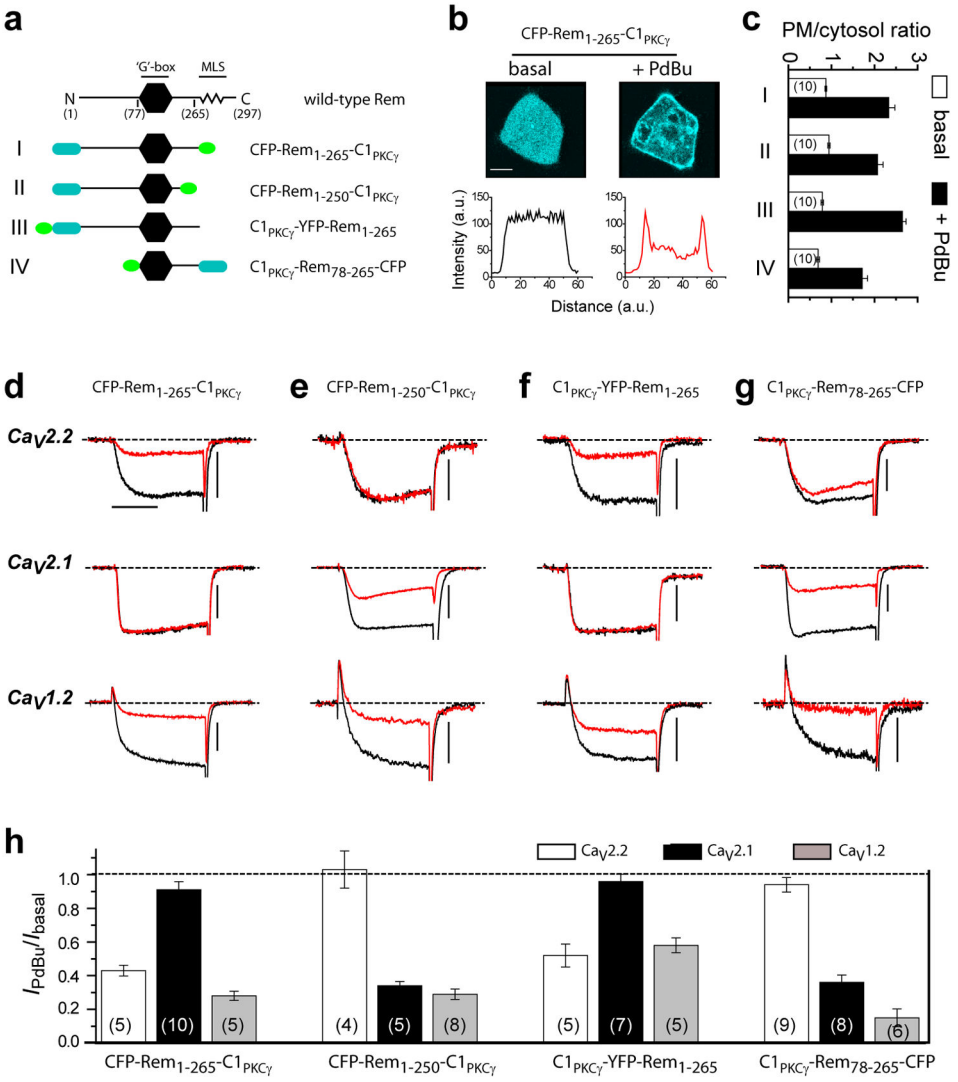


**Figure 1. Placement of membrane-targeting domain influences selectivity and potency of Rem-based $Ca_V1/Ca_V2$ channel blockers**

(**a**) Cartoons of wild-type (wt) Rem and engineered derivatives in which an inducible membrane-targeting $C1_{PKC}$ domain is placed in different positions. Wt Rem contains a guanine nucleotide binding domain (G domain) appended by N and C-terminus extensions. The C-terminus contains a polybasic sequence (MLS) that constitutively targets the protein to the plasma membrane. (**b**) Confocal images (*top*) and line scan plot (*bottom*) showing PdBu-induced translocation of CFP-$Rem_{1–265}$-$C1_{PKC}$ from cytosol to the plasma membrane in a transfected HEK 293 cell. Scale bar, 4μm. (**c**) Bar chart showing PdBu-induced increased plasma membrane to cytosol ratio for all four putative Rem-GEMIICCs. (**d**) Exemplar current waveforms for $Ca_V2.2$ (*top*), $Ca_V2.1$ (*middle*) and $Ca_V1.2$ (*bottom*) channels co-transfected with CFP-$Rem_{1–265}$-$C1_{PKC}$ before (*black trace*) and shortly after (*red trace*) exposure to 1 μM PdBu. Scale bars**,** 400 pA, 10 ms. (**e**, **f**, **g**) Same format as (**d**), but with cells expressing CFP-$Rem_{1–250}$-$C1_{PKC}$, $C1_{PKC}$-YFP-$Rem_{1–265}$, and C1PKC-

Rem78-265-CFP, respectively. (**h**) Population data showing differential impact of distinct Rem-GEMIICCs on $Ca_V2.2$, $Ca_V2.1$, and $Ca_V1.2$ channels. Data are means ± s.e.m.

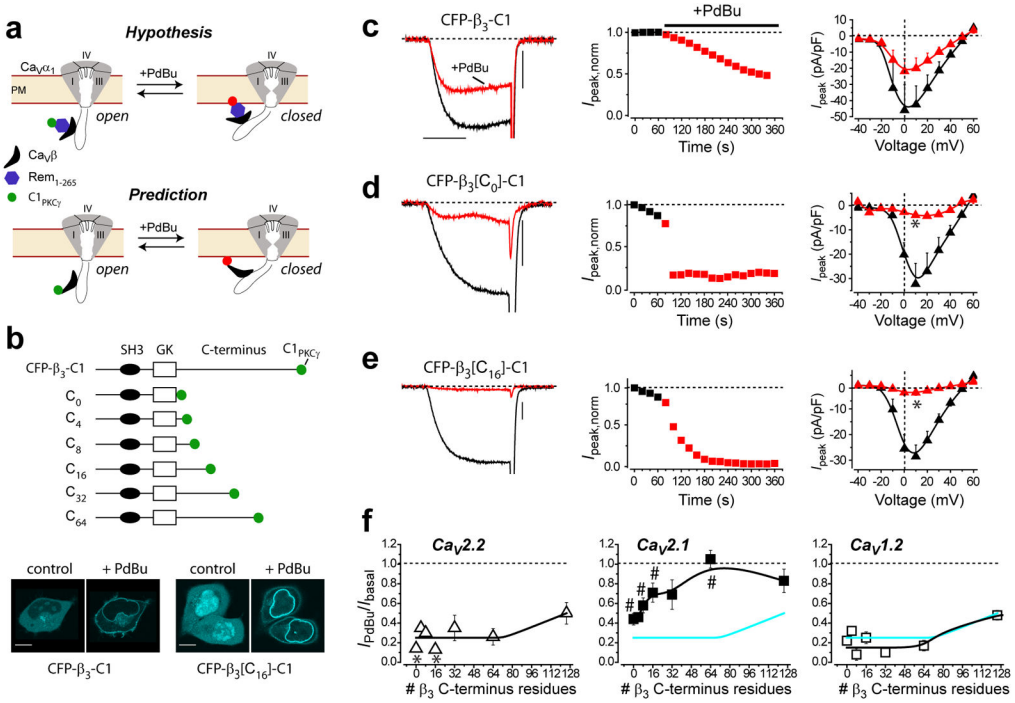


**Figure 2. Design of $Ca_V\beta$-derived CCBs**

(**a**) *Top*, hypothesis for how the dual requirement for membrane-targeting and $Ca_V\beta$-binding translates into Rem inhibition of $Ca_V$ channels. *Bottom*, prediction for creating β-based CCBs. (**b**) *Top*, domain arrangement of $Ca_V\beta_3$ and sites of $C1_{PKC\gamma}$ placement in the C-terminus of serially truncated $Ca_V\beta_3$ subunits. *Bottom*, PdBu-induced translocation of CFP-$\beta_3$-$C1_{PKC\gamma}$ and CFP-$\beta_3[C_{16}]$-$C1_{PKC\gamma}$ from cytosol to plasma membrane. Scale bar, 5 μm. (**c**) *Left*, exemplar currents before (black trace) and after (red trace) exposure to PdBu in HEK 293 cell co-expressing $Ca_V2.2\alpha_{1B}$ and CFP-$\beta_3$-$C1_{PKC\gamma}$. Scale bar, 0.5 nA, 10 ms. *Middle*, diary plot of $I_{Ba}$ amplitude before (black squares) and after (red squares) exposure to 1 μM PdBu. *Right*, population *I–V* curves before (black triangles) and after (red triangles) 1 μM PdBu in cells expressing CFP-$\beta_3$-$C1_{PKC\gamma}$. Data are means ± s.e.m, $n = 6$ for each point. (**d, e**) Data for CFP-$\beta_3[C_0]$-$C1_{PKC\gamma}$ and CFP-$\beta_3[C_{16}]$-$C1_{PKC\gamma}$, respectively; same format as c, $n = 6$ for each point in *I–V* plot. * $P < 0.05$ compared to before PdBu data by two-tailed Student's paired *t* test. (**f**) Normalized $I_{Ca}$ inhibition in HEK 293 cells expressing recombinant $Ca_V2.2$ (white triangles), $Ca_V2.1$ (black squares), or $Ca_V1.2$ (white squares) channels reconstituted with the distinct β-CCBs. Data are means ± s.e.m, $n = 6$ for each point. * significantly different from CFP-$\beta_3$-$C1_{PKC\gamma}$ using one-way ANOVA and Bonferroni test. # $P < 0.05$ compared to $Ca_V2.2$ data (blue line) by two-tailed Student's paired *t* test.

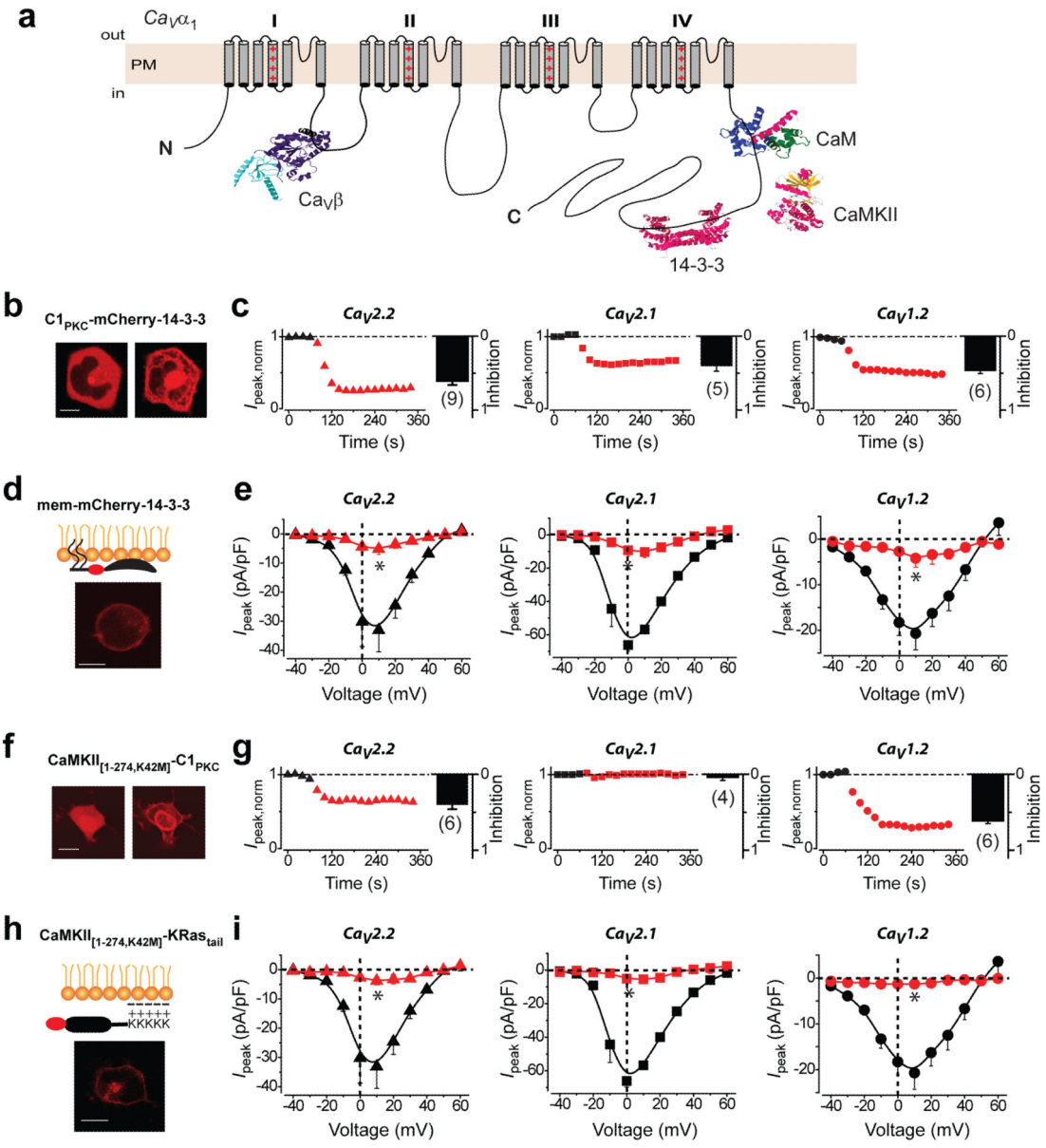


**Figure 3. Generalized method for generating CCBs from $Ca_V\alpha_1$-binding proteins**

(**a**) Schematic of $Ca_V$ channel α1 subunit. Four homologous domains (I–IV) each with six transmembrane segments are joined by intracellular loops and bracketed by cytoplasmic N and C termini. Various proteins bind $Ca_V\alpha1$ intracellular domains including $Ca_V\beta$, 14-3-3, CaM kinase II, and calmodulin. (**b**) Confocal images showing PdBu-induced translocation of $C1_{PKC\gamma}$-mCherry-14-3-3 from the cytosol to the plasma membrane. Scale bar, 4μm. (**c**) Diary plots and population bar charts showing PdBu-induced inhibition of $Ca_V2.2$, $Ca_V2.1$, and $Ca_V1.2$ channels co-expressed with $C1_{PKC\gamma}$-mCherry-14-3-3. Data are means ± s.e.m. (**d**) Schematic and confocal image showing constitutive membrane targeting of mem-mCherry-14-3-3. Scale bar, 5μm. (**e**) Population *I–V* curves showing constitutive inhibition by mem-mCherry-14-3-3 of $Ca_V2.2$ (black triangles, red triangles), $Ca_V2.1$ (black squares, red squares), and $Ca_V1.2$ (black circles, red circles) channels. Data are means ± s.e.m, $n = 5$

for each point. * $P < 0.05$ compared to control data by two-tailed Student's paired *t* test. (**f**) PdBu-induced translocation of mCherry-CaMKII$_{1–274,K42M}$-C1$_{PKC}$ from the cytosol to the plasma membrane. Scale bar, 7μm. (**g**) Diary plots and population bar charts showing PdBu-induced inhibition of $Ca_V2.2$, $Ca_V2.1$, and $Ca_V1.2$ channels co-expressed with mCherry-CaMKII$_{1–274,K42M}$-C1$_{PKC}$. Data are means ± s.e.m. (**h**) Schematic and confocal image showing constitutive membrane targeting of mCherry-CaMKII$_{1–274,K42M}$-KRas$_{tail}$. Scale bar, 5μm. (**i**) Constitutive inhibition of $Ca_V$ channels by mCherry-CaMKII$_{1–274,K42M}$-KRas$_{tail}$. Same format as (**c**). Data are means ± s.e.m, $n = 5$ for each point. * $P < 0.05$ compared to control data by two-tailed Student's paired *t* test.

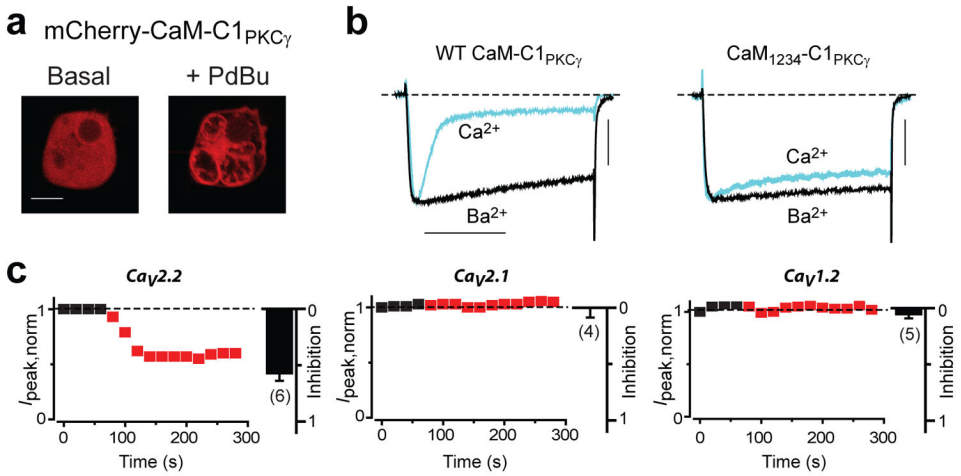


**Figure 4. A CaM based PdBu-inducible CCB selectively inhibits $Ca_V2.2$ channel currents**

(**a**) Confocal image showing PdBu-induced translocation of mCherry-CaM-C1PKC from cytosol to the plasma membrane in a transfected HEK 293 cell. Scale bar, 5 μm. (**b**) The $C1_{PKC}$ tag does not affect the functional interaction of CaM or $CaM_{1234}$ with CaV1.2. Scale bar, 0.5 nA, 10 ms. (**c**) Diary plots and population bar charts showing PdBu-induced effects of $Ca_V2.2$, $Ca_V2.1$ and $Ca_V1.2$ channels co-expressed with mCherry-CaM-$C1_{PKC}$. Data are means ± s.e.m.

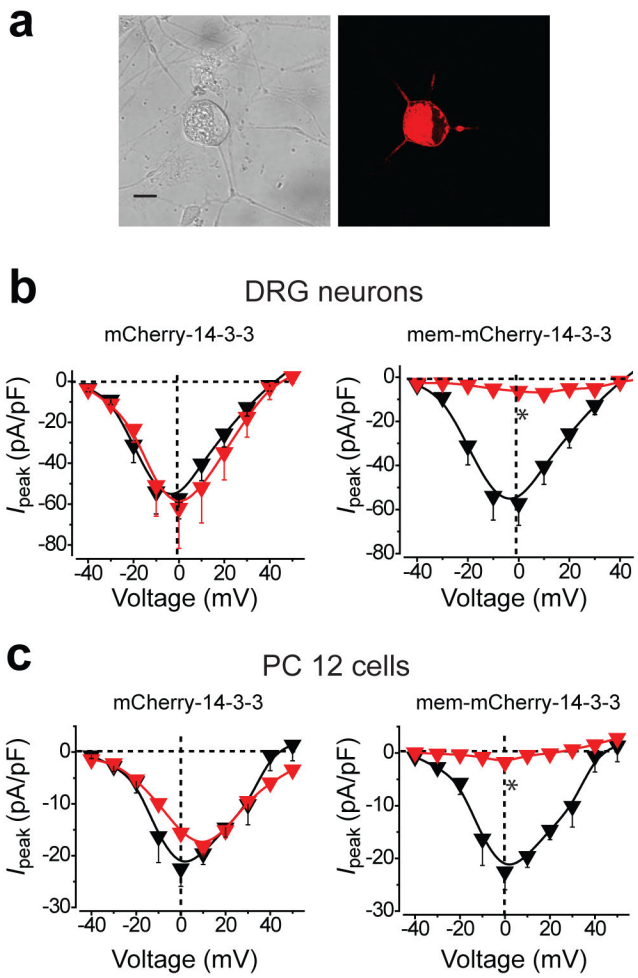


**Figure 5. Constitutive inhibition of endogenous $I_{Ca}$ in native cells with 14-3-3-based CCBs**

(**a**) Greyscale and fluorescence image of DRG neuron expressing mem-mCherry-14-3-3. Scale bar, 5 μm. (**b**) Population *I–V* curves in DRG neurons. Uninfected neurons (black triangles) compared to neurons expressing either mCherry-14-3-3 (*left*) or mem-mCherry-14-3-3 (*right*), $n = 6$ for each point. (**c**) Population *I–V* curves in differentiated PC12 cells, same format as (**b**), $n = 5$ for each point. * $P < 0.05$ compared to control data by two-tailed Student's paired *t* test.

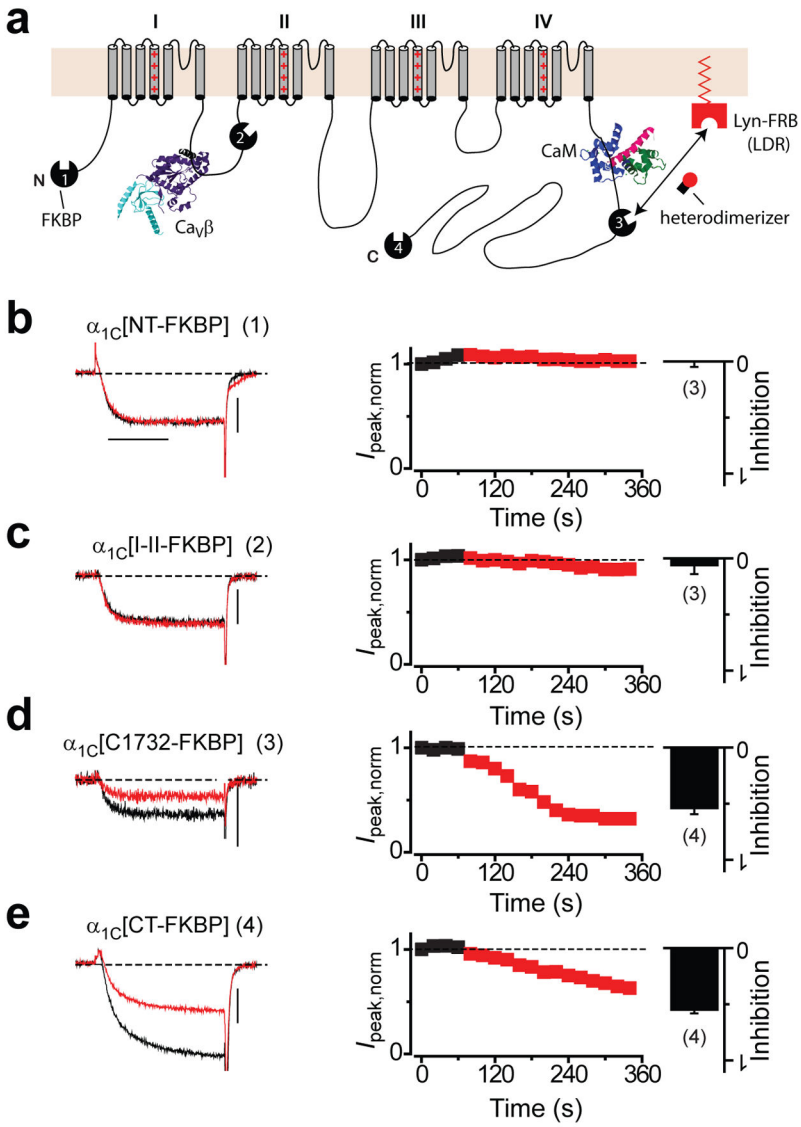


**Figure 6. Principle for developing novel small-molecule CCBs demonstrated using heterodimerization strategy**

(**a**) Insertion of FKBP into selected regions of $\alpha_{1C}$ intracellular loops/termini. **(b–e)** Impact of rapamycin on $I_{Ba}$ from distinct FKBP-fused $\alpha_{1C}$ constructs co-transfected with LDR. Scale bar**,** 400 pA, 10 ms.